HYBRID ANALYSIS OF THE MUTUAL INTERACTION BETWEEN FLOW AND MAGNETIC FIELDS INSIDE A PARALLEL-PLATE CHANNEL

G. E. Assad [1], **gustavo.elia.assad@gmail.com**
J. A. Lima [1], **jalima@cear.ufpb.br**
F.A. Pontes [2], **fabioapbelem@hotmail.com**
E.N. Macêdo [2], **enegrao@ufpa.br**
J.N.N. Quaresma [2], **quaresma@ufpa.br**

[1]Renewable Energy Post-Graduate Program, PPGER/CEAR/UFPB
Federal University of Paraíba, Cidade Universitária, CP 58051-970, João Pessoa, PB, Brazil

[2]Chemical Engineering Post-Graduate Program, PPGEQ/ITEC/UFPA
Federal University of Pará, Campus Universitário do Guamá, CP 66075-110, Belém, PA, Brazil

Abstract. The purpose of the present work is to develop a hybrid analysis of the mutual interaction between flow and magnetic (external and induced) fields of an electric conductive fluid inside a parallel-plate channel. The objective will be achieved with the application of the so-called Generalized Integral Transform Technique (GITT) on the equations that govern the flow of the conductive fluid and the transport of the magnetic field within this flow field. The conductive fluid can enter the channel under any velocity profile and will have its natural development within the channel changed by the applied magnetic field (due to the Lorentz force). Electric currents are induced within the flow and they can be used to power generation, propulsion, levitation and other applications. Due to these electric currents, magnetic fields will also be induced and superposed to that one externally applied. This makes the flow and the magnetic fields strongly coupled. These phenomena add new challenges to the computational method adopted for solution, in view of the presence of new couplings, nonlinearities and boundary conditions for the magnetic field. The study of these interactions will be performed through the two-dimensional Navier-Stokes equations in the stream-function formulation, coupled with the transport equations of the magnetic fields. The choice of the simple geometry is driven by the easy of generation of benchmark results, in contrast to use of a physical model, more difficult to numerical treatment. Results for the main potentials are presented and compared to the literature for various values of the governing parameters. The proposed study placed here falls within the current scenario of use and development of new technologies to alternative sources of energy generation.

Keywords*: MHD (Magnetohydrodynamics), Navier-Stokes Equations, Magnetic Fields, Integral Transforms*

1. INTRODUCTION

Magnetohydrodynamics, or shortly MHD, is the area of science that deals with the interaction between flows of electric conductive fluids and magnetic fields. Mathematically, it seeks for solutions to the coupled equations of electrodynamics and fluid mechanics for typically slow macroscopic interactions between the magnetic field and the fluid flow. In this way the Maxwell's displacement current is neglected and the coupling between equations is through the current density and the generalized Ohm's law. Therefore, the equations of the MHD disregard relativistic corrections, quantum effects, retain mass, energy and momentum.

The flow of electrically conductive fluids within parallel plate channels is the main model used to study the MHD in typical applications. An important work that relates the problem of solution of hydrodynamics entry in the presence of a magnetic field, considering the Navier-Stokes equations, was reported by Brandt and Gillis (1966), who used the streamfunction formulation associated to a finite difference scheme to solve the problem without resorting to any simplifying resources. This reference will be taken as the basis for the present work.

Currently, it is also essential the development and application of mathematical methods that maintain an analytical character in obtaining the solution of equations in various fields of science. Among the methods which satisfy this requirement, at least partially, it is the method known as Generalized Integral Transform Technique - GITT (Cotta, 1993; Cotta, 1998; Santos *et al*., 2001). This is a hybrid numerical-analytical technique that has been developed in parallel to the purely numerical methods and which maintains in its application, all the characteristics of an analytical solution, similar to the variable separation method, associated, on the other hand, to the strength of purely numerical methods for solution of ordinary differential equations. This will be the method adopted in the solution of the problem proposed herein.

Regarding to works that employed the integral transform approach in MHD channel flows, Lima *et al*. (2007) and Lima and Rêgo (2013) were pioneers, although they restricted their attention to the one dimensional unsteady flow or used the boundary layer simplifications, respectively. In an effort to extend those analyses, Pontes *et al*. (2015) studied the developing laminar heat and fluid flow inside a channel considering the two-dimensional version of the Navier-Stokes equations in the streamfunction formulation. Despite of improving the previous hybrid efforts they did not take into account the two-way interaction between the fluid flow field and the magnetic field, *i.e.*, they admitted that the external magnetic field applied in the normal direction to the flow remained uniform, not being influenced by any induced internal magnetic effect inside the magnetically modified flow field.

Therefore, the main objective of the present study is the application of the integral transform approach in order to solve the coupled interaction between both fields (flow and magnetic) in terms of scalar functions for the velocity field (the stream functions, ψ), and for the magnetic field (the magnetic function, β).The physical phenomenon is based on a two-dimensional, incompressible, and steady-state laminar flow of an electric conducting newtonian fluid, inside a parallel plate channel. The mathematical model is obtained from the Navier-Stokes equation and the laws of electromagnetism. The physical properties are constant and the flow is submitted to an external transverse magnetic field, also constant, but that is modified inside the channel while flow is developing. This behavior characterizes a two-way coupled interaction.

2. MATHEMATICAL FORMULATION

Consider a parallel plate channel where the horizontal plates are insulating and the vertical ones are conductors, which consist of electrodes for measuring voltage, current or for connecting a resistive load. An external magnetic field, constant and uniform, $\vec{B}_0^*$, will be transversally imposed in the y^* direction. Inside the channel, the flow influences the development, transport and shape of the magnetic field lines, and which, in turn, reciprocally influence the flow field. Figure 1 shows the main characteristics of the flow, the geometry of the studied problem and its boundary conditions, in its dimensional form[1].

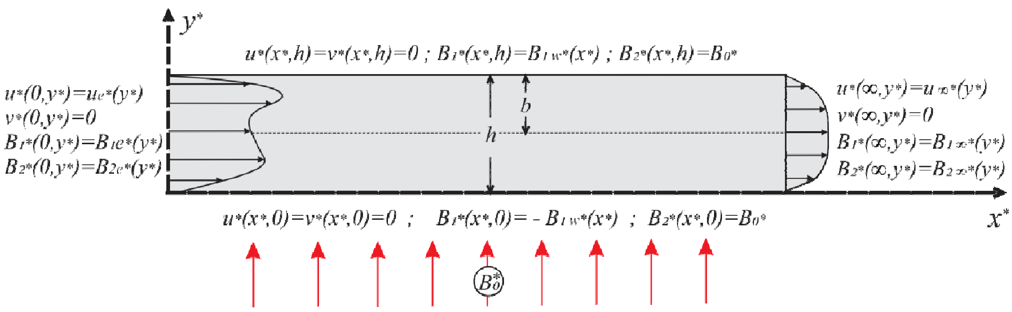

Figure 1: Scheme of the region under study and boundary conditions.

From the simplifications adopted and given a formulation based on the Navier-Stokes equation, the governing equations, in its dimensionless form, can be written as:

$$u\frac{\partial u}{\partial x}+v\frac{\partial u}{\partial y}=-\frac{\partial P}{\partial x}+\frac{1}{\mathrm{Re}}\left(\frac{\partial^2 u}{\partial x^2}+\frac{\partial^2 u}{\partial y^2}\right)-\frac{1}{\mathrm{Re}}J_z B_2 \qquad 0<y<h,\ x>0 \qquad (1)$$

$$u\frac{\partial v}{\partial x}+v\frac{\partial v}{\partial y}=-\frac{\partial P}{\partial y}+\frac{1}{\mathrm{Re}}\left(\frac{\partial^2 v}{\partial x^2}+\frac{\partial^2 v}{\partial y^2}\right)+\frac{1}{\mathrm{Re}}J_z B_1 \qquad 0<y<h,\ x>0 \qquad (2)$$

$$0=\frac{\partial}{\partial y}\left(uB_2-vB_1\right)+\frac{1}{\mathrm{Re}_m}\left(\frac{\partial^2 B_1}{\partial x^2}+\frac{\partial^2 B_1}{\partial y^2}\right) \qquad 0<y<h,\ x>0 \qquad (2)$$

$$0=-\frac{\partial}{\partial x}\left(uB_2-vB_1\right)+\frac{1}{\mathrm{Re}_m}\left(\frac{\partial^2 B_2}{\partial x^2}+\frac{\partial^2 B_2}{\partial y^2}\right) \qquad 0<y<h,\ x>0 \qquad (4)$$

Where the current density, associated to the Lorentz force in the last terms of Eqs. (1) and (2), is given by:

$$J_z=E_z+uB_2-vB_1\equiv\frac{1}{\mathrm{Re}_m}\left(\frac{\partial B_2}{\partial x}-\frac{\partial B_1}{\partial y}\right) \qquad (5)$$

These equations are subjected to following boundary conditions:

$$x=0:\begin{cases}u(0,y)=u_e(y)\\ v(0,y)=0\\ B_1(0,y)=B_{1e}(y)\\ B_2(0,y)=B_{2e}(y)\end{cases},\quad x\to\infty:\begin{cases}u(x\to\infty,y)=u_\infty(y)\\ v(x\to\infty,y)=0\\ B_1(x\to\infty,y)=B_{1\infty}(y)\\ B_2(x\to\infty,y)=B_{2\infty}(y)\end{cases};\quad y=0\begin{cases}u(x,0)=0\\ v(x,0)=0\\ B_1(x,0)=-B_{1w}(x)\\ B_2(x,0)=Ha\end{cases},\quad y=1\begin{cases}u(x,1)=0\\ v(x,1)=0\\ B_1(x,1)=B_{1w}(x)\\ B_2(x,1)=Ha\end{cases} \qquad (5.a\text{-}p)$$

In the above formulation, the following dimensionless groups were employed:

[1] Quantities that present the superscript "*" are dimensional, conversely, quantities that don't present, are dimensionless.

$$x=\frac{x^*}{h}\quad y=\frac{y^*}{h}\quad u=\frac{u^*}{\overline{U}_e}\quad v=\frac{v^*}{\overline{U}_e}\quad P=\frac{P^*}{\rho\overline{U}_e^2}$$
$$b_0=\frac{1}{h}\left(\frac{\mu}{\sigma}\right)^{1/2}{}^{2}\quad B_x=\frac{B_x^*}{b_0}\quad B_y=\frac{B_y^*}{b_0}\quad B_1=\frac{B_1^*}{b_0}=B_x\quad B_2=\frac{B_2^*}{b_0}=B_y+Ha \tag{6.a-o}$$
$$E_z=\frac{E_z^*}{\overline{U}_e b_0}\quad Ha=\frac{B_0^*}{b_0}=B_0^*h\left(\frac{\sigma}{\mu}\right)^{1/2}\quad J_z=\frac{J_z^*}{\sigma\overline{U}_e b_0}\quad Re=\frac{\overline{U}_e h}{\nu}\quad Re_m=\mu_m\sigma\overline{U}_e h=\frac{\overline{U}_e h}{\lambda_m}$$

Here, h is the height of the channel, $\overline{U}_e$ is the average flow velocity at the channel entrance, Ha is the Hartmann number, Re is the Reynolds number, Re_m is the magnetic Reynolds number, λ_m is the magnetic diffusivity, μ_m is the magnetic permeability, σ is the electrical conductivity and E_z is the electric field imposed on the wall-electrodes.

2.2. Formulation in scalar functions

In previous research, which was employed the GITT approach, the use of the stream function formulation showed more pronounced numerical convergence rates than those employing the primitive variable formulation. Thus, considering the following scalar streamfunction and magnetic function,

$$\left(u=\frac{\partial\psi}{\partial y},\ v=-\frac{\partial\psi}{\partial x}\right)\quad\text{and}\quad\left(B_1=\frac{\partial\beta}{\partial y},\ B_2=-\frac{\partial\beta}{\partial x}\right) \tag{7.a-d}$$

Equations (1) to (4), subjected to boundary conditions (5a-p), are now rewritten as:

$$\frac{\partial\psi}{\partial y}\left(\frac{\partial^3\psi}{\partial x^3}+\frac{\partial^3\psi}{\partial x\partial y^2}\right)-\frac{\partial\psi}{\partial x}\left(\frac{\partial^3\psi}{\partial y^3}+\frac{\partial^3\psi}{\partial y\partial x^2}\right)=\frac{1}{\mathrm{Re}}\left(\frac{\partial^4\psi}{\partial x^4}+2\frac{\partial^4\psi}{\partial x^2\partial y^2}+\frac{\partial^4\psi}{\partial y^4}\right)-\frac{1}{\mathrm{Re}\,\mathrm{Re}_m}\left[\frac{\partial\beta}{\partial x}\left(\frac{\partial^3\beta}{\partial x^2\partial y}+\frac{\partial^3\beta}{\partial y^3}\right)-\frac{\partial\beta}{\partial y}\left(\frac{\partial^3\beta}{\partial x^3}+\frac{\partial^3\beta}{\partial x\partial y^2}\right)\right] \tag{8}$$

$$\frac{\partial\psi}{\partial y}\frac{\partial\beta}{\partial x}-\frac{\partial\psi}{\partial x}\frac{\partial\beta}{\partial y}=\frac{1}{\mathrm{Re}_m}\left(\frac{\partial^2\beta}{\partial x^2}+\frac{\partial^2\beta}{\partial y^2}\right)+E_z \tag{9}$$

$$x=0:\begin{cases}\psi(0,y)=g_e(y)\\ \dfrac{\partial\psi}{\partial x}(0,y)=0\\ \beta(0,y)=h_e(y)\end{cases},\qquad x\to\infty\ \begin{cases}\psi(x\to\infty,y)=g_\infty(y)\\ \dfrac{\partial\psi}{\partial x}(x\to\infty,y)=0\\ \beta(x\to\infty,y)=-Ha.x_\infty+h_\infty(y)\end{cases} \tag{10.a-f}$$

$$y=0\ \begin{cases}\psi(x,0)=0\\ \dfrac{\partial\psi}{\partial y}(x,0)=0\\ \beta(x,0)=-Ha.x\end{cases},\qquad y=1\ \begin{cases}\psi(x,1)=1\\ \dfrac{\partial\psi}{\partial y}(x,1)=0\\ \beta(x,1)=-Ha.x+h_\infty(1)\end{cases} \tag{10.g-l}$$

Where $g_\infty(y)$ and $h_\infty(y)$ are functions related to the flow and magnetic fields on the fully developed region (Assad, 2016).

3. SOLUTION METHODOLOGY

3.1. Splitting of scalar functions

The use of the governing equations in terms of scalar functions (ψ and β) reduces the number of equations to be solved, eliminates the terms associated with the pressure and facilitates the numerical solution of the problem. Nevertheless, this formulation still brings non-homogeneous boundary condition, undesirable in the light of the integral transformation approach. To eliminate these non-homogeneities, each original potential is split-up in two parts: a filtered field, which possesses homogeneous boundary conditions, and a filter that carries the original non-homogeneity:

$$\psi(x,y)=\psi_H(x,y)+\psi_F(y),\qquad \beta(x,y)=\beta_H(x,y)+\beta_F(y;x) \tag{11.a,b}$$

---

[b] Note that, in reality, the term b_0 is not dimensionless, rather, it has dimensions of magnetic field. However, it is shown together the dimensionless groups because it is important in the dimensionless process.

In the previous equations, the subscript H is related to the filtered (homogeneous) field and the subscript F is associated to the filter expression. For the streamfunction potential, the filter employed is exactly the solution of the fully developed flow field, $\psi_F(y) = \psi_\infty(y)$. On the other hand, for the magnetic field the filter is an expression that seems similar to the solution of the magnetic field for the fully developed region, differing in the term that takes into account the local axial position being solved. i.e., $\beta_F(y;x) \neq \beta_\infty(y,x_\infty)$. Only for longitudinal positions far from the channel entrance, this filter will equal the expression for the fully developed solution.

$$\psi_F(y) = \psi_\infty(y) = g_\infty(y) \; ; \qquad \beta_F(y;x) = -Ha.x + h_\infty(y) \tag{12.a,b}$$

3.2. Integral Transform

After all boundary conditions in the integral transform direction (y) are made homogeneous, the integral transformation of Eqs. (8-10), after Eqs. (11) and (12), can be performed. The first step is to choose the auxiliary eigenvalue problems that will be used as basis for the eigenfunction expansions. Such eigenvalue problems are obtained from homogeneous versions of the original problems, and are well described in the works of Lima *et al.* (2013), among others. For the streamfunction field, the auxiliary eigenvalue problem has the following properties:

$$\text{Integral Transform / Inverse Pair:} \begin{cases} \bar{\psi}_{Hi}(x) = \displaystyle\int_0^1 \tilde{Y}_i(y)\,\psi_H(x,y)\,\mathrm{dy} \\ \psi_H(x,y) = \displaystyle\sum_{i=1}^{\infty} \tilde{Y}_i(y)\,\bar{\psi}_{Hi}(x) \end{cases} \tag{13}$$

$$\text{Eingenfunctions:} \quad \tilde{Y}_i(y) = \begin{cases} \dfrac{\cos\left[\mu_i\left(y-\frac{1}{2}\right)\right]}{\cos\left(\frac{\mu_i}{2}\right)} - \dfrac{\cosh\left[\mu_i\left(y-\frac{1}{2}\right)\right]}{\cosh\left(\frac{\mu_i}{2}\right)} \; ; \; \mathrm{i} = 1,3,5, \ldots \\ \dfrac{\sin\left[\mu_i\left(y-\frac{1}{2}\right)\right]}{\sin\left(\frac{\mu_i}{2}\right)} - \dfrac{\sinh\left[\mu_i\left(y-\frac{1}{2}\right)\right]}{\sinh\left(\frac{\mu_i}{2}\right)} \; ; \; \mathrm{i} = 2,4,6, \ldots \end{cases} \tag{14}$$

$$\text{The eingenvalues are the roots of: } \cos\mu_i \cosh\mu_i = 1 \; ; \qquad \text{Norm: } \int_0^1 \tilde{Y}_i(y)\tilde{Y}_j(y)\,dy = \begin{cases} N_i = 1\,, & i = j \\ 0\,, & i \neq j \end{cases} \tag{15, 16}$$

Now, for the magnetic field, the eigenproblem has the following properties:

$$\text{Integral Transform/ Inverse Pair:} \begin{cases} \bar{\beta}_i(x) = \displaystyle\int_0^1 \tilde{H}_i(y)\,\beta_H(x,y)\,\mathrm{dy} \\ \beta_H(x,y) = \displaystyle\sum_{i=1}^{\infty} \tilde{H}_i(y)\,\bar{\beta}_i(x) \end{cases} \tag{17}$$

$$\text{Eingenfunctions: } \tilde{H}_i(y) = \frac{H_i(y)}{\sqrt{M_i}} = \sqrt{2}\,\mathrm{sen}(\alpha_i y) \; ; \qquad \text{Eingenvalues: } \alpha_i = i\pi\,, \quad i = 1,2,3,\ldots \tag{18, 19}$$

$$\text{Norm: } M_i = \int_0^1 H_i^2(y)\,dy = \frac{1}{2} \tag{20}$$

The next analytical step of the method is the integral transformation of the governing equation and boundary conditions. This is performed by multiplying each governing equation (Eqs. 8, 9) by its respective eigenfunction (Eqs. 14, 18) and then integrating them in the y direction. Then, after considering the orthogonality properties (Eqs. 16, 20) and the boundary conditions, the following coupled system of ordinary differential equations in the x-direction is obtained, in conjunction with the integral coefficients:

$$\begin{aligned}\frac{d^4\bar{\psi}_{Hi}}{dx^4}(x) = Re&\left\{\begin{aligned}&\sum_{j=1}^{\infty}\sum_{k=1}^{\infty}\left[A_{ijk}^{\psi}\left(\frac{d^3\bar{\psi}_{Hj}}{dx^3}(x)\,\bar{\psi}_{Hk}(x)-\frac{d\bar{\psi}_{Hj}}{dx}(x)\frac{d^2\bar{\psi}_{Hk}}{dx^2}(x)\right)+\left(B_{ijk}^{\psi}-E_{ijk}^{\psi}\right)\frac{d\bar{\psi}_{Hj}}{dx}(x)\,\bar{\psi}_{Hk}(x)\right]\\ &+\sum_{j=1}^{\infty}\left[C_{ij\infty}^{\psi}\frac{d^3\bar{\psi}_{Hj}}{dx^3}(x)+\left(D_{ij\infty}^{\psi}-F_{ij\infty}^{\psi}\right)\frac{d\bar{\psi}_{Hj}}{dx}(x)-\frac{2}{Re}G_{ij}^{\psi}\frac{d^2\bar{\psi}_{Hj}}{dx^2}(x)\right]\end{aligned}\right\}+\\ \frac{1}{Re_m}&\left\{\begin{aligned}&\sum_{j=1}^{\infty}\sum_{k=1}^{\infty}I_{ijk}^{\psi}\left[\frac{d\bar{\beta}_{Hj}}{dx}(x)\frac{d^2\bar{\beta}_{Hk}}{dx^2}(x)-\frac{d^3\bar{\beta}_{Hj}}{dx^3}(x)\,\bar{\beta}_{Hk}(x)+\left(\alpha_j^{\,2}-\alpha_k^{\,2}\right)\frac{d\bar{\beta}_{Hj}}{dx}(x)\,\bar{\beta}_{Hk}(x)\right]+\\ &\sum_{j=1}^{\infty}\left[J_{ijF}^{\psi}\frac{d\bar{\beta}_{Hj}}{dx}(x)+K_{ijF}^{\psi}\left(\frac{d^2\bar{\beta}_{Hj}}{dx^2}(x)-\alpha_j^{\,2}\bar{\beta}_{Hj}(x)\right)+M_{ijF}^{\psi}\left(\alpha_j^{\,2}\frac{d\bar{\beta}_{Hj}}{dx}(x)-\frac{d^3\bar{\beta}_{Hj}}{dx^3}(x)\right)\right]\end{aligned}\right\}\\ &-\left(\mu_i^{\,4}\bar{\psi}_{Hi}(x)+H_{i\infty}^{\psi}-\frac{L_{iFF}^{\psi}}{Re_m}\right)\end{aligned} \tag{21}$$

$$\frac{d^2\bar{\beta}_{Hi}}{dx^2}(x)=\mathrm{Re}_m\left\{\sum_{j=1}^{\infty}\sum_{k=1}^{\infty}\left(A_{ijk}^{\beta}\frac{d\bar{\beta}_{Hj}}{dx}\bar{\psi}_{Hk}-E_{ijk}^{\beta}\bar{\beta}_{Hj}\frac{d\bar{\psi}_{Hk}}{dx}\right)+\sum_{j=1}^{\infty}\left(B_{ijF}^{\beta}\bar{\psi}_{Hj}-F_{ijF}^{\beta}\frac{d\bar{\psi}_{Hj}}{dx}\right)+\sum_{j=1}^{\infty}C_{ij\infty}^{\beta}\frac{d\bar{\beta}_{Hj}}{dx}-\left(H_i^{\beta}E_z-D_{i\infty F}^{\beta}\right)\right\}+\alpha_i^2\bar{\beta}_{Hi}-G_{iF}^{\beta} \tag{22}$$

The inlet and the outlet boundary conditions are equally transformed to yield:

$$\begin{cases}\bar{\psi}_{H_i}(0)=\bar{g}_i=\displaystyle\int_0^1\tilde{Y}_i(y)\,\psi_H(0,y)dy\;=\;\int_0^1\tilde{Y}_i(y)\left[g_e(y)-g_\infty(y)\right]dy\\ \left.\dfrac{d\bar{\psi}_{Hi}}{dx}\right|_{x=0}=0\\ \bar{\beta}_{Hi}(0)=\bar{h}_i=\displaystyle\int_0^1\tilde{H}_i(y)\left[h_e(y)-h_\infty(y)\right]dy\end{cases}\quad,\qquad\begin{cases}\bar{\psi}_{H_i}(x\to\infty)=0\\ \left.\dfrac{d\bar{\psi}_{Hi}}{dx}\right|_{x=\infty}=0\\ \bar{\beta}_{Hi}(x\to\infty)=0\end{cases} \tag{23.a-f}$$

a) For the transformed streamfunction, the coefficients are defined as:

$$A_{ijk}^{\psi}=\int_0^1\tilde{Y}_i(y)\tilde{Y}_j(y)\tilde{Y}_k^{'}(y)dy \qquad B_{ijk}^{\psi}=\int_0^1\tilde{Y}_i(y)\tilde{Y}_j^{''}(y)\tilde{Y}_k^{'}(y)dy \qquad C_{ij\infty}^{\psi}=\int_0^1\tilde{Y}_i(y)\tilde{Y}_j(y)\frac{d\psi_\infty(y)}{dy}dy$$

$$D_{ij\infty}^{\psi}=\int_0^1\tilde{Y}_i(y)\tilde{Y}_j^{''}(y)\frac{d\psi_\infty(y)}{dy}dy \qquad E_{ijk}^{\psi}=\int_0^1\tilde{Y}_i(y)\tilde{Y}_j(y)\tilde{Y}_k^{'''}(y)dy \qquad F_{ij\infty}^{\psi}=\int_0^1\tilde{Y}_i(y)\tilde{Y}_j(y)\frac{d^3\psi_\infty(y)}{dy^3}dy$$

$$G_{ij}^{\psi}=\int_0^1\tilde{Y}_i(y)\tilde{Y}_j^{''}(y)dy \qquad H_{i\infty}^{\psi}=\int_0^1\tilde{Y}_i(y)\frac{d^4\psi_\infty(y)}{dy^4}dy \qquad I_{ijk}^{\psi}=\int_0^1\tilde{Y}_i(y)\tilde{H}_j(y)\tilde{H}_k^{'}(y)dy$$

$$J_{ijF}^{\psi}=\int_0^1\tilde{Y}_i(y)\tilde{H}_j(y)\frac{\partial^3\beta_F(y;x)}{\partial y^3}dy \qquad K_{ijF}^{\psi}=\int_0^1\tilde{Y}_i(y)\tilde{H}_j^{'}(y)\frac{\partial\beta_F(y;x)}{\partial x}dy \qquad L_{iFF}^{\psi}=\int_0^1\tilde{Y}_i(y)\frac{\partial\beta_F(y;x)}{\partial x}\frac{\partial^3\beta_F(y;x)}{\partial y^3}dy$$

$$M_{ijF}^{\psi}=\int_0^1\tilde{Y}_i(y)\tilde{H}_j(y)\frac{\partial\beta_F(y;x)}{\partial y}dy \tag{24.a-m}$$

b) And for the transformed magnetic function

$$A_{ijk}^{\beta}=\int_0^1\tilde{H}_i(y)\tilde{H}_j(y)\tilde{Y}_k^{'}(y)dy \qquad B_{ijF}^{\beta}=\int_0^1\tilde{H}_i(y)\tilde{Y}_j^{'}(y)\frac{\partial\beta_F}{\partial x}(y;x)dy \qquad C_{ij\infty}^{\beta}=\int_0^1\tilde{H}_i(y)\tilde{H}_j(y)\frac{d\psi_\infty}{dy}(y)dy$$

$$D_{i\infty F}^{\beta}=\int_0^1\tilde{H}_i(y)\frac{d\psi_\infty}{dy}(y)\frac{\partial\beta_F}{\partial x}(y;x)dy \qquad E_{ijk}^{\beta}=\int_0^1\tilde{H}_i(y)\tilde{H}_j^{'}(y)\tilde{Y}_k(y)dy \qquad F_{ijF}^{\beta}=\int_0^1\tilde{H}_i(y)\tilde{Y}_j(y)\frac{\partial\beta_F}{\partial y}(y;x)dy$$

$$G_{iF}^{\beta}=\int_0^1\tilde{H}_i(y)\frac{\partial\beta_F^2}{\partial y^2}(y;x)dy \qquad H_i^{\beta}=\int_0^1\tilde{H}_i(y)dy \tag{25.a-h}$$

These coefficients were evaluated through Gaussian quadrature by using the routine QDAGS from the IMSL package (IMSL, 2010). A criterion of 10^{-12} was used as relative error target for each coefficient. Additionally, since the length along the channel to reach the fully developed condition, x_∞, is not known '*a priori*', the following change of coordinates is implemented in the numerical procedure to transform the domain from x: $[0, x_\infty]$ to domain η: [0, 1]:

$$\eta = 1 - e^{-cx}, \qquad \frac{d\eta}{dx} = 1 - \eta \tag{26.a,b}$$

In these expressions, c is a contraction scale factor, a positive parameter that governs the amount of contraction imposed to the coordinate.

3. RESULTS AND DISCUSSION

To obtain the numerical results, a computer code was developed in FORTRAN 90 language. From the IMSL package (IMSL, 2010), subroutine BVPFD, which is especially suitable for solving systems of stiff ordinary differential equations, was employed to solve the coupled system, Eqs. (21-24). A relative error target of 10^{-4} was employed as criterion for convergence of the transformed potentials.

First of all, a convergence analysis is performed for the longitudinal velocity component at the center of the channel, $u_c(x)$, for the upper-wall velocity gradient, $\partial u/\partial y|_{y=1} \equiv f_x\,Re/2$, and for the difference of the magnetic function between the channel centerline and the wall, $\Delta\beta(x)$, at different longitudinal positions and physical parameters.

$$\Delta\beta(x) = \beta(x, 0.5) - \beta(x, 1) \tag{27}$$

Tables 1 illustrates the convergence behavior of these potentials for Re = 20; Ha = 2; E_z = -2 and different values of magnetic Reynolds number (Re_m =10^{-4}, 1 and 50). In addition to the convergence behavior, an exam of this table also reveals the influence of the coupling parameter between flow and magnetic field, *i.e.*, the magnetic Reynolds number, Re_m, on the flow and magnetic fields development. In these tables, $N = N\psi = N\beta$ is the number of terms employed in the expansions for the streamfunction and the magnetic function series.

Table 1. Convergence behavior of some potentials in different axial positions, for Re = 20, Ha = 2, E_0 = -2

$Re_m = 10^{-4}$

N \ x	$u_c(x)$					$\partial u/\partial y\|_{y=1} \equiv f_x\,Re/2$					$\frac{\Delta\beta(x)}{Re_m}$ x 10^2				
	0.1	0.2	0.3	0.4	x_∞	0.1	0.2	0.3	0.4	x_∞	0.1	0.2	0.3	0.4	x_∞
5	1.108	1.097	1.149	1.224	1.476	18.95	14.51	11.22	9.179	6.389	0.8479	1.624	2.404	3.139	6.051
10	1.012	1.082	1.163	1.244	1.476	25.73	14.13	10.08	8.390	6.389	0.8276	1.661	2.481	3.230	6.051
30	1.022	1.082	1.164	1.246	1.476	24.30	13.15	9.798	8.288	6.389	0.8269	1.671	2.494	3.243	6.051
50	1.021	1.082	1.163	1.246	1.476	23.73	13.09	9.784	8.283	6.389	0.8269	1.671	2.495	3.243	6.051

$Re_m = 1$

N \ x	$u_c(x)$					$\partial u/\partial y\|_{y=1} \equiv f_x\,Re/2$					$\frac{\Delta\beta(x)}{Re_m}$ x 10^2				
	0.1	0.2	0.3	0.4	x_∞	0.1	0.2	0.3	0.4	x_∞	0.1	0.2	0.3	0.4	x_∞
5	1.108	1.476	1.476	1.476	1.476	18.95	14.50	11.22	9.170	6.389	0.6695	5.986	6.046	6.051	6.051
10	1.012	1.082	1.163	1.245	1.476	25.73	14.12	10.07	8.380	6.389	0.6442	1.346	2.081	2.787	6.051
30	1.022	1.082	1.164	1.246	1.476	24.30	13.14	9.790	8.278	6.389	0.6428	1.355	2.094	2.801	6.051
50	1.021	1.082	1.164	1.246	1.476	23.73	13.09	9.776	8.273	6.389	0.6429	1.355	2.094	2.801	6.051

$Re_m = 50$

N \ x	$u_c(x)$					$\partial u/\partial y\|_{y=1} \equiv f_x\,Re/2$					$\frac{\Delta\beta(x)}{Re_m}$ x 10^2				
	0.1	0.2	0.3	0.4	x_∞	0.1	0.2	0.3	0.4	x_∞	0.1	0.2	0.3	0.4	x_∞
5	1.108	1.097	1.150	1.228	1.476	18.94	14.48	11.18	9.114	6.389	0.06565	0.06851	0.09513	0.1548	6.051
10	1.012	1.083	1.164	1.248	1.476	25.72	14.10	10.05	8.345	6.389	0.01293	0.03076	0.07982	0.1556	6.051
30	1.022	1.082	1.165	1.249	1.476	24.29	13.13	9.772	8.250	6.389	0.005352	0.02993	0.08150	0.1581	6.051
50	1.022	1.082	1.165	1.249	1.476	23.73	13.08	9.758	8.245	6.389	0.005359	0.02994	0.08150	0.1581	6.051

From this table, one clearly observes the strong convergence rates for the selected potentials obtained with the integral transform approach, *i.e.*, with only few terms (N = 10) a convergence in the third digits is already attained.

Now, results obtained with the present methodology are compared with the numerical results of Brandt and Gillis (1966), who employed the finite difference method to analyze the same problem through the same formulation. To verify the code developed, comparisons are initially performed for the case of non-MHD flows (Ha = 0) for different Reynolds numbers. Figure 2.a and 2b show these comparisons by illustrating the development of the longitudinal velocity along the channel for Re = 20 and Re = 500, respectively.

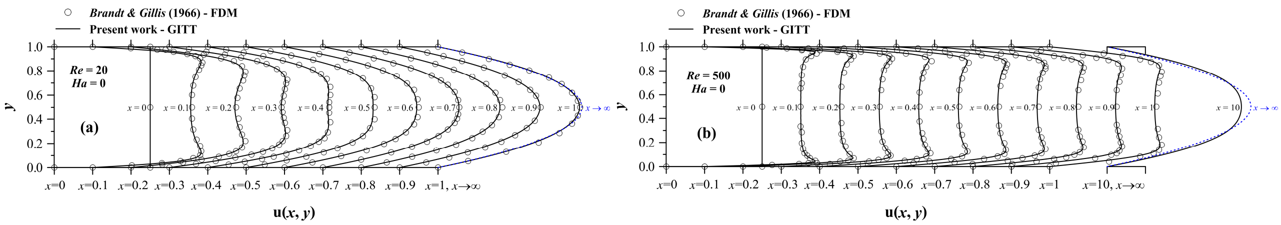

Figure 2 – Development of the axial velocity component profile for Ha = 0: a) Re = 20 and b) Re = 500.

These figures show the strong effect of the Reynolds number on the flow development along the channel axis. The greater the Reynolds number the flatter is the profile of the longitudinal component velocity, making, as expected, the wall velocity gradient much more elevated. Another interesting feature visualized on these figures is the well-known pronounced M-shape (concavity) of the velocity profile at the inlet region, especially for higher Reynolds number. This effect is not captured in the boundary layer formulation, being the explained by the additional term of axial diffusion of momentum present in the Navier-Stokes formulation.

On its turn, Figure 3.a and 3.b illustrate the behavior of the longitudinal velocity component profiles along the x-axis for different magnetic Reynolds numbers (Re_m = 10^{-4} and Re_m = 50, respectively). For the first case, comparisons are still performed with the results of Brandt and Gillis (1966).

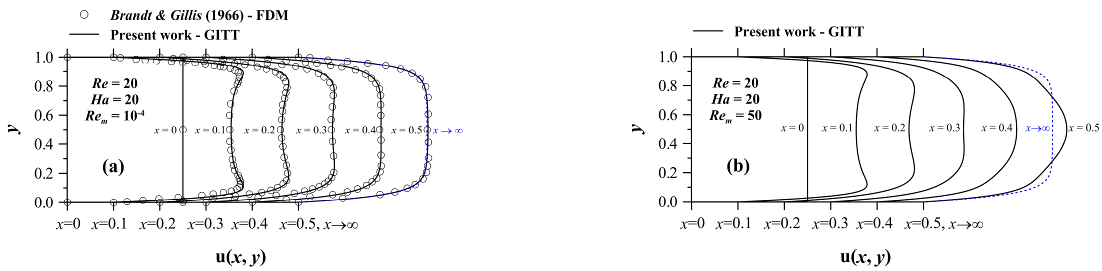

Figure 3 – Development of the axial velocity component profile for Re = 20, Ha = 20: a) Re_m = 10^{-4} and b) Re_m = 50.

From these figures, it seems that the effect of the magnetic Reynolds number is more intense in a region after some distance from the inlet and before the exit of the channel. Apparently, it seems that the flow development is not perturbed by the magnetic field when they are nearby the channel inlet (x = 0.1 and x = 0.2). Maybe, in this region, the induced magnetic field is not strong enough to alter the characteristic of the flow field. It also is interesting to note that the development of the centerline velocity presents an overshooting behavior along the channel for increasing magnetic Reynolds number.

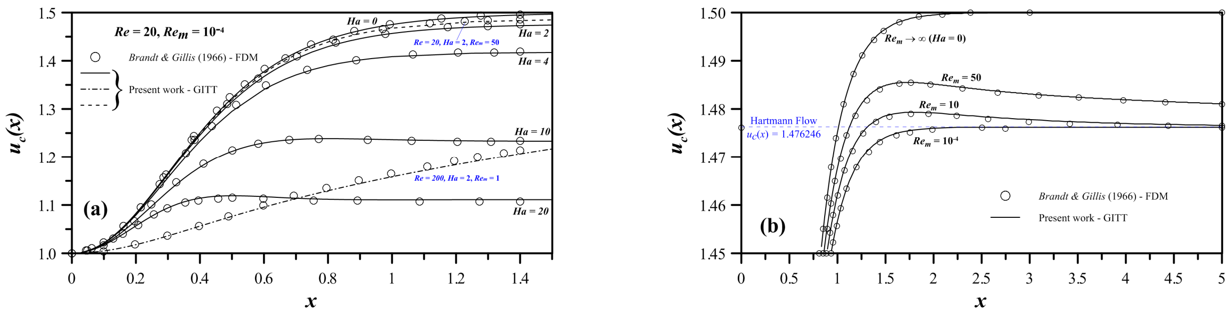

Figure 4 – Development of the centerline velocity for Re = 20 and, a) Re_m = 10^{-4} and various values of Ha. Dashed curve is for Re = 20, Ha = 2 and Re_m = 50. Dash-dot curve is for Re = 200, Ha = 2 and Re_m = 1; b) Ha = 2 and various values of Re_m. The curve marked $Re_m \rightarrow \infty$ is for Ha = 0.

According to Fig. (3.b), the centerline velocity increases from axial positions from 0 to 0.5 and then decreases to the fully developed value. This could be explained as follows: as the flow is developing, the vertical component of the magnetic field is reduced and the axial component is increased, the same happens with the longitudinal and vertical components of the Lorentz force. Therefore, the flow field, nearby the centerline, is less influenced by the longitudinal component of the Lorentz force, and its magnitude increases.

To better clarify this behavior, Fig. 4 illustrates the development of the centerline velocity component along the channel for values of Hartmann and magnetic Reynolds number. Figure 4.a illustrates the development for Re = 20, $Re_m = 10^{-4}$ and different values of the Hartmann number, Ha. Figure 4.b shows the development for Re = 20, Ha = 2 and different values of the magnetic Reynolds number, Re_m. These figures clearly shows that, for increasing Ha and Re_m, the overshooting phenomenon is established, confirming the previous statements about Fig. 3.

Finally, the behavior of development of the magnetic field is illustrated in Fig. 5, through the difference of the magnetic function between the channel centerline and the wall, $\Delta\beta(x)$. For improvement of visualizations this variable is plotted normalized by the magnetic Reynolds number, Re_m.

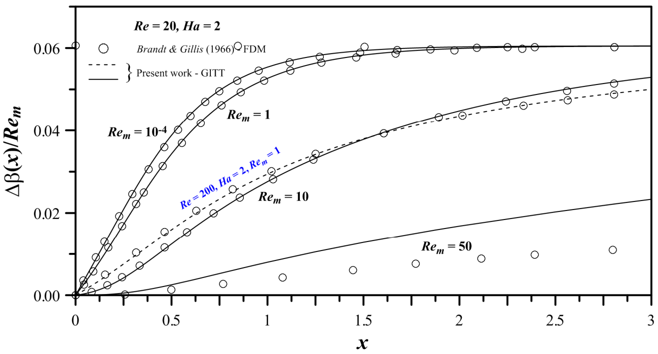

Figure 5 – Development of magnetic scalar function on the centerline. Solid curves are for Re = 20, Ha = 2 and various values of Re_m. The dashed curve is for Re = 200, Ha = 2 and Re_m = 1.

3. CONCLUSIONS

The Generalized Integral Transform Technique (GITT) was successfully applied in the solution of the coupled flow and magnetic fields inside a parallel-plate channel. Its main hybrid characteristics and numerical behavior were analyzed and results were compared with, previously reported, numerical data for different values of the governing parameters. It should be here emphasized that, at least to the authors knowledge, no works that employed the integral transform approach as the mathematical tool for solving the governing equations have considered the coupled phenomenon in its full MHD formulation (the Navier-Stokes equations coupled to electromagnetism ones). Therefore, the present works represents an advance in the methodology application. An extension of the present work, taking into account the forced convection and different magnetic boundary conditions (for magnetohydrodynamic generator or motor), is presently in preparation.

5. REFERENCES

Brandt, A. & Gillis, J., 1966. “Magnetohydrodynamic Flow in the Inlet Region of a Straight Channel”. The Physics of Fluids, vol. 9, no 4, p. 690-699.

Cotta, R.M., 1993. “Integral transform in computational heat and fluid flow”. CRC PRESS, Boca Raton, FL, USA.

Cotta, R.M. 1998. “The Integral Transform Method in Thermal and Fluid**”.** Science and Engineering, Begell House Inc, NY, USA.

IMSL Library, Math/Lib., Houston, TX, 2010.

Lima, J.A.; Quaresma, J.N.N. and Macêdo, E.N., 2007. “Integral transform analysis of MHD flow and heat transfer in parallel-plates channels”. International Communications in Heat and Mass Transfer, vol. 34, n. 4, pp. 420-431.

Lima, J.A.; Rêgo, M.G.O., 2013. “On the integral transform solution of low-magnetic MHD flow and heat transfer in the entrance region of a channel”. International Journal of Non-Linear Mechanics, vol. 50, 2013, p.25-39.

Pontes, F.A.; Macêdo, E.N.; Batista, C.S.; Lima, J.A. and Quaresma, J.N.N., 2015. “Integral transform solution for magnetohydrodynamic flow whith heat transfer in a parallel-plate channel”. International Congress of Mechanical Engineering – COBEM2015, Rio de Janeiro, RJ, Brazil.

Santos, C.A.C.; Quaresma, J.N.N. & Lima, J.A., 2001. Convective Heat Transfer in Ducts: The Integral Transform Approach. *E-Papers*, 348 p., ABCM Mecanical Sciences Series, Rio de Janeiro, RJ, Brazil.